

Critical behavior in an atomistic model for a bistable surface reaction: CO oxidation with rapid CO diffusion

N. Pavlenko,^{1,*} R. Imbühl,¹ J. W. Evans,^{2,3} and Da-Jiang Liu²

¹*Institut für Physikalische Chemie und Elektrochemie, Universität Hannover, Callinstrasse 3-3a, D-30167 Hannover, Germany*

²*Ames Laboratory, Iowa State University, Ames, Iowa 50011, USA*

³*Department of Mathematics, Iowa State University, Ames, Iowa 50011, USA*

(Received 11 February 2003; published 15 July 2003)

We analyze critical behavior associated with the loss of bistability for an atomistic model for CO oxidation on surfaces in the limit of infinite diffusion of CO. The model includes infinite nearest-neighbor repulsions between adsorbed immobile O. We use a “hybrid” treatment incorporating a lattice-gas description of the O adlayer, but tracking just the number of adsorbed CO (which are randomly distributed on non-O sites). The critical exponents obtained from a finite-size-scaling analysis on $L \times L$ site surfaces with periodic boundary conditions show that the “hybrid” reaction model belongs to the mean-field universality class, despite strong spatial correlations in the O adlayer. We also quantify finite-size effects in the global bifurcation diagram, revealing a significant shift of the bistable region with decreasing system size. Our study elucidates fluctuation effects observed in experiments of CO oxidation on the nanoscale facets of metal-field emitter tips.

DOI: 10.1103/PhysRevE.68.016212

PACS number(s): 05.45.-a, 05.10.-a, 82.65.+r, 05.40.-a

I. INTRODUCTION

Many studies of catalytic surface reactions in recent years have focused on bridging the “materials gap” between traditional ultrahigh vacuum surface science analyses on extended single-crystal substrates and industrial catalysis typically involving nanoscale supported metal clusters [1]. The question of how to appropriately model catalytic reactions is by no means trivial due to the very different length and time scales involved.

On the *mesoscale*, behavior of catalytic reactions on extended single-crystal substrates is well understood. Rapid diffusion of some adspecies ensures efficient local mixing facilitating application of mean-field (MF) rate equations to effectively describe hysteresis and bifurcation behavior [2], and MF reaction-diffusion equations to describe pattern formation on the scale of several microns [3]. On the *nanoscale*, catalytic reactions have been studied on supported metal nanoclusters using conventional techniques [4,5], on the nanofacets of metal field emitter tips (FET’s) with field electron/ion microscopy [6,7], and on single-crystal surfaces with scanning tunneling microscopy [8]. However, here fluctuations may generate new effects not predicted by deterministic MF rate or reaction-diffusion equations. Fluctuation-induced transitions between the two states of a bistable system may occur for reactions on FET’s or supported metal clusters [6,7,9], and bifurcation behavior can be modified, e.g., shifting bistable regions and cusp points. The general topic of fluctuation effects in finite bistable reaction systems has been explored extensively at the MF level using master equations, stochastic rate equations, or associated Fokker-Planck equations [10–13].

On surfaces, strong interactions between adsorbed particles may lead to islanding or superlattice ordering in the adlayer [14]. These effects, in addition to limited mobility of some adspecies, can generate strong spatial correlations in reactant adlayers. While conventional MF formulations cannot treat these effects, they may be accurately described by atomistic lattice-gas (LG) models [15,16]. Furthermore, for reactions in nanoscale systems, such as the facets of a FET, which contain only a few hundred to a few thousand adsorption sites, LG modeling is an ideal tool to analyze the role of both spatial correlations and fluctuations [5–7]. A *basic question* is whether fluctuation effects in LG modeling differ qualitatively from predictions of MF treatments. To address this issue, in this paper, we naturally focus on analyzing *critical behavior* near a bifurcation point where fluctuations are amplified.

Specifically, we will consider LG models for CO oxidation, which incorporate the appropriate Langmuir-Hinshelwood mechanism (reversible adsorption of CO at single empty sites, irreversible dissociative adsorption of O₂ at suitable pairs of empty sites, reaction of adjacent adsorbed CO and O). The earliest treatment of this type was the classic Ziff-Gulari-Barshad (ZGB) model [17], which ignored diffusion and desorption of adsorbed CO, implemented O₂ adsorption on nearest-neighbor (NN) empty sites, and neglected all adsorbate interactions. We modify this model to include desorption and rapid diffusion of adsorbed CO, and a refined treatment of O₂ adsorption reflecting strong interactions between neighboring adsorbed O [6,18,19]—all of which are important features in the reaction.

Some key aspects of the behavior in these CO oxidation models for infinite systems are independent of their finer details [16], as we now describe. For *low CO mobility* [16,17], there is a discontinuous transition from a reactive state (with low CO coverage) to an inactive or near-CO-poisoned state (with high CO coverage) upon increasing CO partial pressure, provided the CO desorption rate is small. Metastability and hysteresis are weak. The discontinu-

*Present address: Institut für Theoretische Physik, Physik-Department der TU München, James-Frank St., D-85747 Garching, Germany.

ous transition disappears at a “critical point” upon increasing CO desorption. For *high (or infinite) CO mobility* [16,18], this discontinuous transition is replaced by bistability (corresponding to strong hysteresis observed in experiments), so the system can exist either in a stable reactive state or in a stable inactive state. The region of the bistability terminates at the critical cusp bifurcation point upon increasing CO desorption.

For either low or high mobility, fluctuation amplitudes increase dramatically upon approaching the (nonequilibrium) critical point, analogous to behavior near the critical point in equilibrium systems. However, precise determination of critical behavior is nontrivial. Despite the apparent analogy between equilibrium and nonequilibrium behavior, a complete correspondence is not possible due to the absence of a free energy and the lack of detailed balance in nonequilibrium systems. Nevertheless, recent LG studies of nonequilibrium critical behavior successfully employed some key concepts and techniques from equilibrium studies [universality classes, finite-size scaling (FSS)] [20–24]. Of particular significance is a study by Tomé and Dickman [20], which showed that critical behavior in a ZGB-type model for CO oxidation with *immobile* adsorbed CO (and O), but including CO desorption, was described by the Ising universality class. However, typically hop rates for diffusing CO are many orders of magnitude greater than other relevant rates (for adsorption, desorption, and reaction), so of more practical relevance is the determination of critical behavior for *rapid (or infinite) CO diffusion*. Above we noted the development of MF-type bistability with increasing CO mobility [16,18]. This might suggest MF (rather than Ising) critical behavior. However, a careful analysis of fluctuation behavior near the critical point is needed to confirm this speculation.

Thus, in the present work, we analyze critical behavior in a “hybrid” LG model for CO oxidation, which treats directly behavior in the limit of infinite CO mobility. In Sec. II, we describe this model and the associated coverage distributions (or histograms), which adopt a bimodal form in the bistable region. The latter are characterized in terms of a Landau-type effective potential or free energy, facilitating a precise finite-size scaling analysis. In Sec. III, we report our results for critical exponents, which assume MF values despite strong spatial correlations in the O adlayer, and also analyze the finite-size shifts of the global bifurcation diagrams. In Sec. IV, we compare our results with traditional MF behavior, and discuss more general models for CO oxidation with finite CO mobility. We also note that many aspects of fluctuation behavior studied here are accessible in experiments on FET’s. However, FET’s involve multiple facets which are not isolated, but rather “weakly” coupled by CO diffusion, and this impacts size-scaling behavior (see Appendix B).

II. HYBRID REACTION MODEL AND COVERAGE DISTRIBUTIONS

We now describe the “hybrid” lattice-gas model for CO oxidation [6,18,24] employed for this study. We use square lattices of $L \times L$ adsorption sites with periodic boundary con-

ditions. Below, (gas) and (ads) denote gas and adsorbed states, respectively.

(i) CO(gas) adsorbs onto single empty sites at the rate p_{CO} per site, and desorbs at the rate d . CO(ads) hops to nearby empty sites, and here we consider only the regime of infinitely mobile CO(ads). We also neglect interactions between CO(ads) and other CO(ads) and O(ads), so the distribution of CO(ads) on sites not occupied by O(ads) is random. Thus, it suffices to adopt a “hybrid” simulation procedure [18,25], where we track only the total number of CO(ads), but incorporate a full lattice-gas description of the distribution of O(ads).

(ii) O₂(gas) adsorbs dissociatively at the impingement rate p_{O_2} per site. To account for very strong NN O(ads)-O(ads) repulsions, we invoke an “eight-site rule” [26,27] wherein O₂(gas) adsorbs only at diagonal NN empty sites, provided that the additional six sites adjacent to these are not occupied by O(ads). Also, O(ads) is immobile, cannot desorb, and thus never occupies adjacent sites of the lattice.

(iii) Adjacent pairs of CO(ads) and O(ads) react at the rate k to form CO₂(gas), which desorbs immediately.

As in previous studies, we set $p_{\text{CO}} + p_{\text{O}_2} = k = 1$ and consider system behavior as a function of $p = p_{\text{CO}}$ with $p_{\text{O}_2} = 1 - p_{\text{CO}}$. For our analysis, we define the coverage of adsorbed species of the type $J = \text{CO (O)}$ as $\theta_J = N_J / L^2$, where N_J is the number of the adsorbed CO (O) particles. The time-averaged steady-state coverages are denoted by $\langle \theta_J \rangle$.

To place this study in a broader context, one could consider a LG model for CO oxidation, which differs from the hybrid model only through incorporation of a finite CO hop rate h . Such a model is characterized by a diffusion length, $R_{\text{diff}} \sim h^{1/2}$, for large h . Thus, our hybrid treatment lets $R_{\text{diff}} \rightarrow \infty$ at the outset (and in certain analyses *subsequently* lets $L \rightarrow \infty$). Therefore, the hybrid model always treats the regime where $L \ll R_{\text{diff}}$.

The key quantity considered in our analysis is a reduced version of the steady-state distribution $P(N_{\text{CO}}, N_{\text{O}})$, describing the joint probability of having N_{CO} CO(ads) and N_{O} O(ads) on the surface [28]. In terms of $P(N_{\text{CO}}, N_{\text{O}})$, average coverages can be written as

$$\langle \theta_J \rangle = \sum_{N_{\text{CO}}, N_{\text{O}}} \theta_J P(N_{\text{CO}}, N_{\text{O}}). \quad (1)$$

Further, one can consider reduced distributions such as

$$P(N_{\text{CO}}) = \sum_{N_{\text{O}}} P(N_{\text{CO}}, N_{\text{O}}),$$

so that

$$\langle \theta_{\text{CO}} \rangle = \sum_{N_{\text{CO}}} \theta_{\text{CO}} P(N_{\text{CO}}). \quad (2)$$

When the parameters (p, d) correspond to the bistable region (for a given L), the distributions $P(N_{\text{CO}}, N_{\text{O}})$ and $P(N_{\text{CO}})$ are bimodal, with the two peaks corresponding to the reactive and inactive states [28]. To recover this behavior in

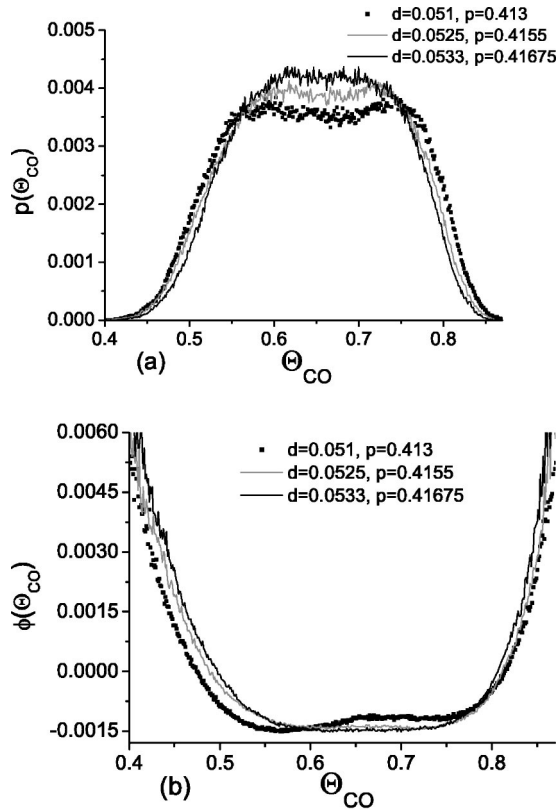


FIG. 1. (a) Probability distribution for the CO coverage in the hybrid reaction model with $L=30$; (b) the corresponding effective potential.

simulation data, one must analyze time series for the coverages for sufficiently long times that the system can make many noise-induced transitions between these states. In describing the behavior of the reaction model, it is helpful to draw analogy with equilibrium magnetic systems. Roughly speaking, the CO desorption rate d is a temperature-like variable, and p_{CO} is an external field-like variable. For infinite (large) systems, bistability (or hysteresis) occurs for a range of p values when $d < d_c$, the critical value of the CO desorption rate, and disappears when $d > d_c$. Correspondingly, for finite (small) systems, $P(N_{\text{CO}}, N_0)$ should exhibit a transition from bimodal to monomodal distribution at $d_c(L)$, which, in general, depends on L . In Fig. 1(a), we show this behavior for $P(N_{\text{CO}})$ for $L=30$: two peaks are evident for $d=0.051$ and $d=0.0525$ [below $d_c(L)=0.0531$], but only one peak for $d=0.0533$ [above $d_c(L)$]. The value of p_{CO} is chosen to be at the “midpoint” of the bistable region [for $d < d_c(L)$] so that the distributions $P(N_{\text{CO}})$ is near symmetric. However, unlike in the magnetic systems, there is no explicit symmetry so that one can easily identify the “midpoint” of the bistable or bimodal region, and the distribution is generally asymmetric even at the midpoint.

Clearly, a challenge in our study of the criticality of CO oxidation is the need to locate the critical point in the two-dimensional (2D) (p, d) -parameter space. Further, this must be done for various L in our finite-size-scaling analyses. Also, computationally efficient histogram reweighting methods, applicable for equilibrium systems [29], do not apply

due to the lack of a free energy. It is apparent that we need an optimum strategy to analyze noisy data for probability distributions such as $P(N_{\text{CO}})$ (for various L) to precisely discern the subtle transition from a bimodal to monomodal form. To this end, it will be convenient to introduce an effective potential (mimicking a thermodynamic free energy) defined by [11–13,28]

$$\phi_L(\theta_{\text{CO}}) = -L^{-2} \ln \rho_L(\theta_{\text{CO}}), \quad (3)$$

where $\rho_L(\theta_{\text{CO}}) = L^2 P(N_{\text{CO}})$ is normalized under integration over continuous coverage variable θ_{CO} as $L \rightarrow \infty$. Also, $\phi_L(\theta_{\text{CO}})$ has a “weak” L dependence, but converges to a well-defined limiting form as $L \rightarrow \infty$. From Eq. (3), $\rho_L(\theta_{\text{CO}}) = \exp[-L^2 \phi_L(\theta_{\text{CO}})]$ adopts a Boltzmann-like form, so clearly the effective potential ϕ_L has a double-well form in the bistable regime, the minima corresponding to the stable states [12,28] (see, Sec. III A for more details).

III. FINITE-SIZE-SCALING RESULTS

A. Finite-size shift in the critical point and the shift exponent λ

Our goal here is to determine the behavior as $L \rightarrow \infty$ of the coordinates $(p_c(L), d_c(L))$ of the cusp point in the (p_{CO}, d) plane. It is expected that the shift of the critical point due to finite system sizes has a scaling form [30]

$$d_c(L) - d_c(\infty) \sim L^{-\lambda}$$

and

$$p_c(L) - p_c(\infty) \sim L^{-\lambda}, \quad (4)$$

as $L \rightarrow \infty$, where λ is the shift exponent. Most commonly, $\lambda = 1/\nu$, where ν is the correlation exponent [30]. For the 2D Ising model, $\nu = 1$. Tomé and Dickman [20] show that $\lambda = 1$ for the (zero CO mobility) ZGB model modified to incorporate CO desorption, and conclude that the nonequilibrium reactive-inactive transition belongs to the Ising universality class.

Our procedure to locate the critical (or cusp) point (for each L) involves analysis of simulation data for the effective potential (3), which we fit by adopting a quartic Landau-type form [31]

$$\phi_L(\theta_{\text{CO}}) \approx a_0 + a_1 \delta\theta_{\text{CO}} + a_2 (\delta\theta_{\text{CO}})^2 + a_4 (\delta\theta_{\text{CO}})^4, \quad (5)$$

where $\delta\theta_{\text{CO}} = \theta_{\text{CO}} - \theta_{\text{CO}}^S$, and the “symmetric” coverage θ_{CO}^S is determined by requiring vanishing of the cubic term in the expansion of $\phi_L(\theta_{\text{CO}})$. The parameter θ_{CO}^S and also the coefficients a_i depend on d and p_{CO} (as well as on L). One natural way to define the critical point $[p_c(L), d_c(L)]$ for finite L is to require $a_1 = a_2 = 0$.

More specifically, our procedure (for each L) includes the following steps.

(a) For a given d value (and some selected p_{CO}), from the probability distribution (2), we obtain the effective potential (3) and fit to the quartic form (5) to obtain θ_{CO}^S and a_i .

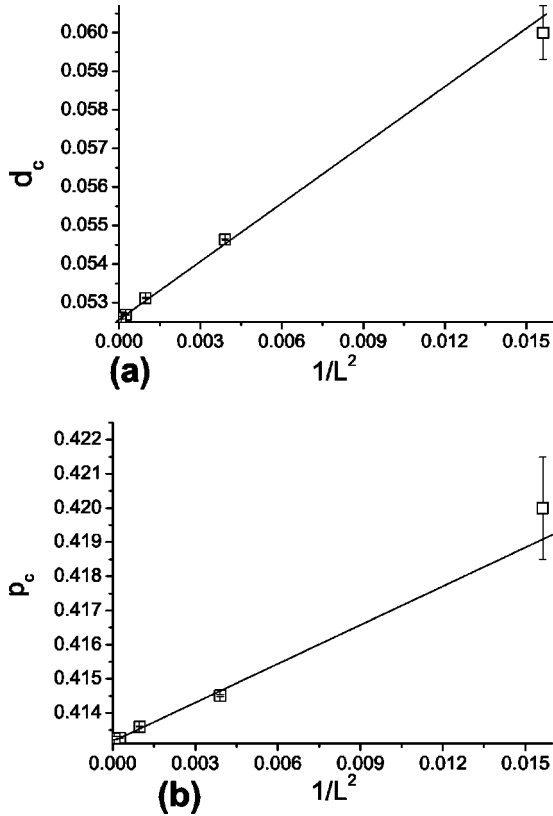


FIG. 2. (a) d_c and (b) p_c vs $1/L^2$ for $L=8-128$ with linear fit corresponding to $\lambda=2$.

(b) Repeat (a) for different p_{CO} to obtain $a_1(p_{CO}, d)$ versus p_{CO} . Determine the p_{CO} value where $a_1(p_{CO}, d)=0$ and denote it by p_{CO}^{eq} . Record the corresponding value for a_2 as $a_2^{eq}(d)$.

(c) Repeat (a) and (b) for various d to find where $a_2^{eq}(d)=0$. Then, with $d=d_c(L)$, steps (a) and (b) give $p_{CO}=p_c(L)$ when $a_1(p_{CO}, d_c(L))=0$.

Our approach here is similar to that used by Orkoulas, Fisher, and Panagiotopoulos [32] in a recent study of criticality in equilibrium fluid systems. Other systematic approaches of locating “equistability” or “symmetry” loci in a two-parameter plane are also considered in that work. The equistability-type condition $a_1(p_{CO}^{eq}, d)=0$ gives approximately an equal-height two-peak distribution in $P(N_{CO})$. In Appendix A, we discuss alternative prescriptions for p_{CO}^{eq} .

In Fig. 2, we plot as a function of $1/L^2$ the finite-size critical values $p_c(L)$ and $d_c(L)$ obtained using the procedure described above. Values of $d_c=0.5464(2)$, $0.5312(2)$, $0.05269(2)$, $0.05262(3)$ and $p_c=0.41451(3)$, $0.41360(2)$, $0.41327(3)$, $0.41326(4)$ for $L=16, 32, 64, 128$, respectively, are fit very well by Eq. (4) with $\lambda=2$, and yield estimates of $d_c=0.0526$ and $p_c=0.4132$ for $L\rightarrow\infty$. The $\lambda=2$ result is in clear contrast to that of Tomé and Dickman [20] for immobile adsorbates. It agrees with the prediction of a MF population model, as discussed further below. This suggests that our “hybrid” CO oxidation model for infinite CO mobility exhibits MF behavior. However, one should also check other critical exponents.

TABLE I. Critical exponents obtained from finite-size-scaling analysis. Uncertainties: ± 0.03 .

L	γ	β
8	0.98	0.51
16	0.99	0.50
32	1.01	0.49
64	1.00	0.49

B. Critical exponents β and γ

Denoting $t=(d-d_c)$, a physical quantity K_L (e.g., suitable order parameters, fluctuation amplitudes) that exhibits algebraic singularity in infinite systems, i.e., $K_\infty\sim t^{-\rho}$, satisfies the following FSS form:

$$K_L\sim L^{\rho\theta}f(tL^\theta), \quad (6)$$

with $f(x)\sim x^{-\rho}$ for $x\gg 1$, and where θ is an exponent measuring the rounding of the singularity due to finite-size effects. Standard FSS hypothesis predicts $\theta=1/\nu$; however, for MF critical behavior, it can be shown that $\theta=D/2$ [33], where D is the dimensionality of the system. Nonetheless, for $D=2$, both the Ising (where $\nu=1$) and the MF behavior give $\theta=1$. Therefore, we have when $t=0$,

$$\chi_L\equiv L^2(\langle\theta_{CO}^2\rangle-\langle\theta_{CO}\rangle^2)\sim L^\gamma \quad (7)$$

and

$$M_L\equiv\langle|\theta_{CO}-\langle\theta_{CO}\rangle|\rangle\sim L^{-\beta}, \quad (8)$$

where $\gamma=1$ and $\beta=1/2$ for the MF criticality, and $\gamma=3/2$ and $\beta=1/8$ for the Ising criticality in two dimensions.

We have performed extensive simulations to determine M_L and χ_L for different system sizes, $L=8, 16, \dots$. Then, utilizing values for pairs of sizes L_1 and L_2 , the critical exponents in the limit $d\rightarrow d_c$ (or $t\rightarrow 0$) are estimated from

$$\beta=\frac{\ln M_{L_1}-\ln M_{L_2}}{\ln L_2-\ln L_1},$$

$$\gamma=\frac{\ln \chi_{L_1}-\ln \chi_{L_2}}{\ln L_1-\ln L_2}. \quad (9)$$

Table I shows the results calculated from Eq. (9), using $L_1=L_2/2=L$. Note that the values obtained for $\beta(\gamma)$ lie close to 0.5 (1.0), which is consistent with MF behavior.

C. Finite-size shift in global bifurcation diagrams

Rather than just identifying the cusp point (p_c, d_c) , a global bifurcation diagram maps out the region of bistability $p_-(d)<p=p_{CO}<p_+(d)$, for each $d<d_c$, where $p_-(d)$ and $p_+(d)\rightarrow p_c$, as $d\rightarrow d_c$ (from below). The finite-size shift of the cusp point coordinates shown in Fig. 2 implies a finite-size shift of the entire bifurcation diagram, a feature that we will quantify here. First, we provide a more detailed characterization of behavior at p_\pm . For fixed $d<d_c$, the bimodal

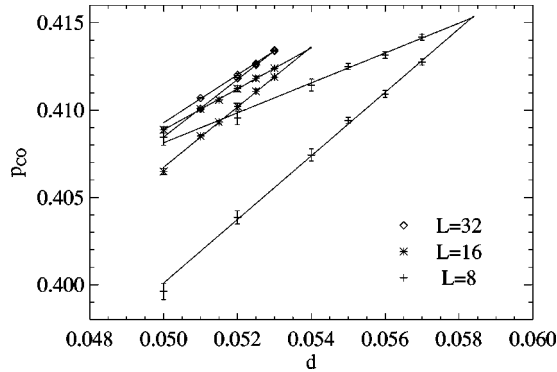


FIG. 3. Bifurcation diagrams showing the bistable region in the hybrid reaction model for various L .

probability distribution $\rho_L(\theta_{\text{CO}})$ becomes increasingly asymmetric as one approaches the boundaries of the bistable region, one of the two maxima disappearing at p_{\pm} . Correspondingly, the effective potential $\phi_L(\theta_{\text{CO}})$ also becomes more asymmetric, one of the two wells disappearing at p_{\pm} . Thus, the following efficient procedure to determine p_{\pm} can be developed based on our quartic fits (5) to $\phi_L(\theta_{\text{CO}})$.

First, we note that as one crosses out of the bistable region, there is a transition from three local extrema (two minima and one maxima) to one local extremum (a minimum) in $\phi_L(\theta_{\text{CO}})$. Correspondingly, there is a transition from three real roots to one real root of the cubic polynomial equation

$$d\phi_L(\theta_{\text{CO}})/d\theta_{\text{CO}} \approx a_1 + 2a_2\delta\theta_{\text{CO}} + 4a_4(\delta\theta_{\text{CO}})^3 = 0. \quad (10)$$

This transition is conveniently signaled by a change in sign (from positive to negative) of the polynomial discriminant,

$$D_3 = -\frac{1}{2}\left(\frac{a_2}{a_4}\right)^3 - \frac{27}{16}\left(\frac{a_1}{a_4}\right)^2 = \frac{1}{2}\left|\frac{a_2}{a_4}\right|^3 - \frac{27}{16}\left(\frac{a_1}{a_4}\right)^2, \quad (11)$$

given that $a_2 < 0$ in the bistable region (and $a_4 > 0$). The increase in asymmetry of $\phi_L(\theta_{\text{CO}})$, as quantified by $|a_1|$, causes the second term to grow and eventually dominate the first term in D_3 . Thus, specifically, our procedure for each $d < d_c$ is to determine $a_i(p_{\text{CO}})$, and thus $D_3(p_{\text{CO}})$, for several values of p_{CO} . Then, we estimate p_{\pm} from the requirement that $D_3(p_{\text{CO}} = p_{\pm}) = 0$. As an aside, we note that for the discussion in Sec. III A, it was convenient to choose a ‘‘symmetric’’ coverage that reduced $\phi_L(\theta_{\text{CO}})$ to a form where the cubic term was absent. However, for the current analysis, this yields no computational advantage. The general form of $\phi_L(\theta_{\text{CO}})$ including a cubic term produces a quadratic term in Eq. (10). However, the edges of the bistable region are still indicated by vanishing of the appropriate discriminant for this more general cubic polynomial, although the interpretation of this discriminant is less transparent than in Eq. (11).

In Fig. 3, we plot the calculated regions of bistability for $L = 8, 16$, and 32 . The striking size effect observed here is a substantial expansion of the bistable region with decreasing L , showing the importance of the large fluctuations in small-

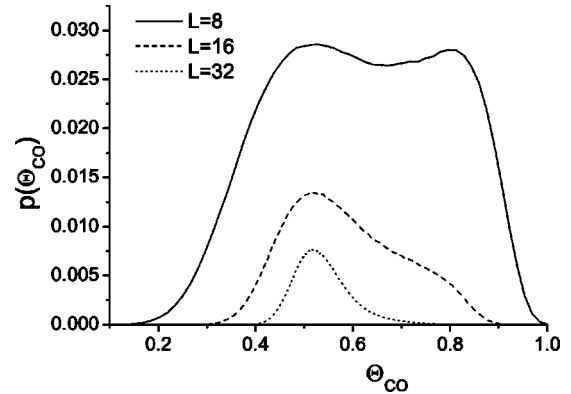


FIG. 4. Probability distribution for the CO coverage when $d = 0.053$ and $p_{\text{CO}} = 0.410$ for various L .

size systems. This effect is reflected in Fig. 4 where the size-induced evolution of the reduced probability distribution is shown at a fixed point ($d = 0.053, p_{\text{CO}} = 0.410$) in parameter space, exhibiting a transition from the bistable state for $L = 8$ to the stable reactive state with the lower CO coverage for $L = 32$. It should be noted that there exist previous detailed studies of finite-size shifts in bifurcation diagrams for bistable systems, but only at the MF level [10].

IV. CONCLUSIONS AND DISCUSSION

We have studied criticality in a ‘‘hybrid’’ lattice-gas model for CO oxidation incorporating infinite diffusion of adsorbed CO. The results for the critical exponents obtained from a finite-size-scaling analysis show that this model belongs to the mean-field universality class, despite the strong spatial correlations in the O adlayer. This behavior is consistent with observed bistability for the hybrid reaction model in infinite systems [18], and with the persistence of a double-well effective potential as $L \rightarrow \infty$ (for $d < d_c$) [28]. This contrasts behavior for reaction models with immobile adsorbates, which exhibit Ising criticality, and where the double-well nature of the effective potential disappears as $L \rightarrow \infty$ (for $d < d_c$). The above differences demonstrate the importance of incorporating (realistic) rapid CO diffusion in modeling CO oxidation on surfaces.

Furthermore, we see that the presence of rapid diffusion validates (at least qualitatively) traditional MF studies (using master equations, Langevin-type rate equations, or Fokker-Plank equations) of noise effects in nanoscale reaction systems. Such studies based on MF master equations provide detailed insight into the effective potential (at least for single variable systems), and reveal a system size dependence of the form [34]

$$\phi_L(\theta_{\text{CO}}) = \phi^0(\theta_{\text{CO}}) + L^{-2}\phi^1(\theta_{\text{CO}}) + \dots \quad (12)$$

Form (12) is consistent with finite-size scaling of form (4) with $\lambda = 2$. Furthermore, we reiterate that such studies have been exploited to characterize analytically finite-size shifts in the bifurcation diagram [10,12], producing results similar to those presented in Sec. III C. Finally, we note that this result is obtained in situations where boundary effects are mini-

mized (e.g., using periodic boundary conditions). For a realistic alternative scenario, see Appendix B.

For a more comprehensive understanding of the critical behavior in LG models for CO oxidation, it is natural to explore behavior in a modified version of the model considered here, which incorporates a finite CO hop rate h . As noted in Sec. II, such a model is characterized by a diffusion length $R_{\text{diff}} \sim h^{1/2}$ for large h . It is thus tempting to make an analogy with equilibrium LG models with attractive interactions (or ferromagnetic Ising-type models) where the interaction range R_{int} is variable. In such equilibrium models, one finds a crossover from Ising to MF critical behavior with increasing R_{int} [35]. Thus, one might expect a corresponding crossover in reaction models with increasing R_{diff} . Such a correspondence is confirmed by an analysis using more refined finite-size-scaling procedures, presented in detail elsewhere [36]. See also Ref. [37] for sample results for the case $h=2$.

It is worth noting that using the Landau-type form of effective potential Eq. (5) does not bias us toward MF results even though the Landau free energy is the basis for MF theories of phase transitions. Using the same approach, we demonstrate Ising behavior for the reaction model with finite (small) CO diffusion [37]. Utility of this approach is further demonstrated in the numerical study of equilibrium phase transitions [see Eq. (2.21) of Ref. [32]].

Finally, we recall that our study of finite-size effects on fluctuations and critical behavior in $L \times L$ site nanoscale reaction systems was motivated by the experimental studies of CO oxidation on metal FET's [6,7]. Such studies can probe many aspects of the coverage distributions explored here (e.g., variation of asymmetry upon scanning the bistable region, dependence on system size, scaling approaching d_c). However, in reality, such FET's consist of several nanoscale facets of different orientations and reactivities for which the reaction is at least weakly coupled by interfacet diffusion of CO [6,7,38]. Such coupling leads to additional finite-size shifts in cusp points and bifurcation diagrams. Since these could be as significant as the fluctuation-induced shifts discussed above, we provide some analysis of these effects in Appendix B for a simple two-facet model. Our approach here in locating the critical point of finite systems proves to be quite effective even in situations where statistics of simulations data is limited (compared with what can be achieved in equilibrium systems). The approach, therefore, can also be used for experimental studies.

ACKNOWLEDGMENTS

N.P. gratefully acknowledges support of this research by the Alexander von Humboldt Foundation and thanks the Ames Laboratory for providing computational facilities. D.J.L. and J.W.E. were supported for this work by the Division of Chemical Sciences, USDOE, through Ames Laboratory (operated by for the USDOE by Iowa State University under Contract No. W-7405-Eng-82).

APPENDIX A: DETERMINATION OF EQUISTABILITY IN FINITE SYSTEMS

In our determination of the critical point in Sec. III A for systems with finite size L , we first locate an "equistability"

pressure $p_{\text{CO}}^{\text{eq}}(d)$ inside the bistable region $p_- \leq p_{\text{CO}} \leq p_+$ based on one specific criterion. This approximately corresponds to equal peak heights (for $d < d_c$) for $P(N_{\text{CO}})$. We then monitor behavior as $d \rightarrow d_c$. It should be noted that various nonequivalent criteria exist for $p_{\text{CO}}^{\text{eq}}(d)$ when $d < d_c(L)$, e.g., equal peak heights for $P(N_{\text{CO}})$ versus equal populations of the two stable states. However, as $L \rightarrow \infty$, all reasonable choices converge more rapidly than critical finite-size effects. For our analysis, the specific choice is not important, as one just needs some consistent recipe to approach the critical point from within the bistable region.

We note that for bistable CO oxidation models with finite

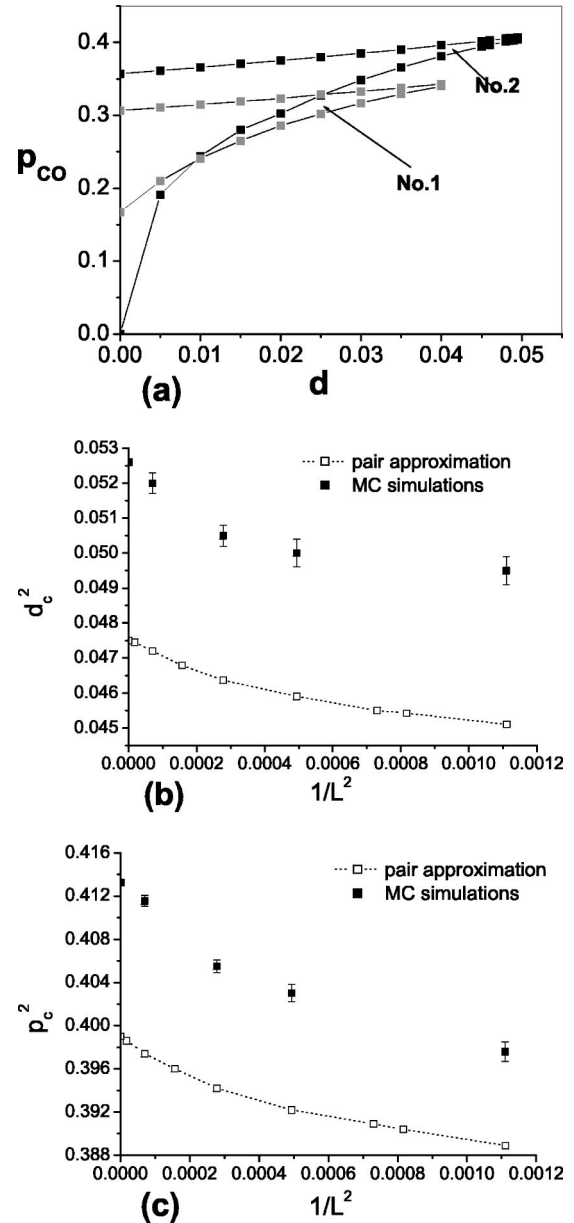


FIG. 5. (a) Bifurcation diagrams showing two bistable regions for the two-facet hybrid reaction model with $L=60$; (b) d_c^2 and (c) p_c^2 vs $1/L^2$ for the two-facet hybrid reaction model for $L=30-120$. Solid squares are simulation results, while open squares correspond to analytic results within the pair approximation.

diffusion length R_{diff} , there is a different equistability criterion, based on stationarity of planar chemical wave separating the two stable states in systems with $L \gg R_{\text{diff}}$ [16,39–41]. At first glance, there is an apparent mismatch between the two criteria. The criterion based on stationarity of planar chemical wave depends on the details of CO diffusion (e.g., coverage dependence) [16], while the criterion based on equal-height distribution is insensitive to the details of CO diffusion for $L \ll R_{\text{diff}}$. However, the equistability based on the equal-height distribution will depend on details of CO diffusion when $L \gtrsim R_{\text{diff}}$, and we expect the two criteria to match when $L \gg R_{\text{diff}}$ [16].

APPENDIX B: TWO-FACET CO OXIDATION MODEL

As in Ref. [38], we extend the hybrid reaction model to a system of two facets, labeled $i=1,2$, both of size $L \times L$ adsorption sites with periodic boundary conditions. These have the same reaction parameters, except for different oxygen sticking coefficients, s_{O}^1 and s_{O}^2 , and are coupled by CO-diffusion. Assume that diffusive transfer of CO from facet i to j occurs by hopping at microscopic rate h_{micro} of CO at the edge of facet i across a common boundary of length L to empty edge sites on facet j . Then, the corresponding rate of gain of θ_{CO}^i from interfacet diffusion satisfies $d/dt \theta_{\text{CO}}^i (i \rightarrow j) \approx h_{ij} \theta_{\text{CO}}^i (1 - \theta_{\text{CO}}^i - \theta_{\text{CO}}^j)$, where the interfacet transport rate $h_{ij} = h_{\text{micro}}/L$ has an explicit L dependence [38]. When $s_{\text{O}}^1 = 0.7$, $s_{\text{O}}^2 = 1.0$, and $h_{\text{micro}} = 0.6$, the bifurcation diagram of

the entire system for large L exhibits two bistable regions, region j corresponding to two stable states with very different θ_{CO}^j [see Fig. 5(a)].

To determine the size-dependent critical points (p_c^1, d_c^1) and (p_c^2, d_c^2) terminating bistability regions 1 and 2 in the (p_{CO}, d) plane, we perform an analysis of the $P(N_{\text{CO}}^i)$ analogous to Sec. III A. Figures 5(b, c) show results for p_c^2 and d_c^2 vs $1/L^2$, depicted by full squares. Since $h_{ij} \rightarrow 0$, for $L \rightarrow \infty$, the interfacet coupling becomes negligible, and the values $p_c^2(L)$ and $d_c^2(L)$ approach the single-facet values p_c and d_c for the infinite L . However, we note the strong nonlinear variation with L^{-2} for smaller sizes, $L < 60$, and that $p_c^2(L)$ and $d_c^2(L)$ increase with increasing L , both features contrasting the behavior in the single-facet case.

We claim that both these features are deterministic in origin, reflecting the L dependence of the diffusive coupling. This L dependence dominates the fluctuation-mediated linear scaling with L^{-2} observed for a broad range of L in the single-facet case. Support for this claim comes from the analysis of the deterministic rate equations for facet coverages obtained in a Kirkwood-type pair approximation, but including coupling due to interfacet diffusion [38]. Results are shown in Figs. 5(b, c) together with the exact behavior. The variation of $p_c^2(L)$ and $d_c^2(L)$ with L is qualitatively similar to the “exact” simulation results, the shift in absolute values occurring because the pair approximation does not exactly recover the cusp point for infinite L .

-
- [1] *Surface Science of Catalysis*, Vol. 482 of ACS Symposium Series, American Chemical Society, edited by D.J. Dwyer and F.M. Hoffmann (American Chemical Society, Washington, DC, 1992).
- [2] R. Imbihl and G. Ertl, *Chem. Rev.* (Washington, D.C.) **95**, 697 (1995).
- [3] G. Ertl, *Adv. Catal.* **37**, 213 (1991).
- [4] L.F. Razon and R.A. Schimtz, *Catal. Rev. - Sci. Eng.* **28**, 89 (1986).
- [5] V.P. Zhdanov and B. Kasemo, *Surf. Sci. Rep.* **39**, 25 (2000).
- [6] Y. Suchorski, J. Beben, E.W. James, J.W. Evans, and R. Imbihl, *Phys. Rev. Lett.* **82**, 1907 (1999).
- [7] Y. Suchorski, J. Beben, R. Imbihl, E.W. James, D.-J. Liu, and J.W. Evans, *Phys. Rev. B* **63**, 165417 (2001).
- [8] S. Völkening, K. Bedürftig, K. Jacobi, J. Winterlin, and G. Ertl, *Phys. Rev. Lett.* **83**, 2672 (1999).
- [9] V.P. Zhdanov and B. Kasemo, *Surf. Sci.* **496**, 251 (2002).
- [10] W. Ebeling and L. Schimansky-Geier, *Physica A* **98**, 587 (1979).
- [11] P. Hänggi, P. Talkner, and M. Borkovec, *Rev. Mod. Phys.* **62**, 251 (1990).
- [12] H. Malchow and L. Schimansky-Geier, *Noise and Diffusion in Bistable Nonequilibrium Systems* (Teubner-Verlag, Leipzig, 1986), Chap. 3.
- [13] C.W. Gardiner, *Handbook of Stochastic Methods for Physics, Chemistry and the Natural Sciences* (Springer-Verlag, Berlin, 1983), Chap. 9.
- [14] T. Engel and G. Ertl, *Adv. Catal.* **28**, 1 (1979).
- [15] S. Völkening and J. Winterlin, *J. Chem. Phys.* **114**, 6382 (2001).
- [16] J.W. Evans, D.-J. Liu, and M. Tammaro, *Chaos* **12**, 131 (2002).
- [17] R.M. Ziff, E. Gulari, and Y. Barshad, *Phys. Rev. Lett.* **56**, 2553 (1986).
- [18] E.W. James, C. Song, and J.W. Evans, *J. Chem. Phys.* **111**, 6579 (1999).
- [19] V.P. Zhdanov and B. Kasemo, *Surf. Sci.* **412/413**, 527 (1998).
- [20] T. Tomé and R. Dickman, *Phys. Rev. E* **47**, 948 (1993).
- [21] C.A. Voigt and R.M. Ziff, *Phys. Rev. E* **56**, R6241 (1997).
- [22] J. Marro and R. Dickman, *Nonequilibrium Phase Transitions in Lattice Models* (Cambridge University Press, Cambridge, 1999).
- [23] H. Hinrichsen, *Adv. Phys.* **49**, 815 (2000).
- [24] D.-J. Liu and J.W. Evans, *Phys. Rev. Lett.* **84**, 955 (2000).
- [25] M. Tammaro, M. Sabella, and J.W. Evans, *J. Chem. Phys.* **103**, 10277 (1995).
- [26] S.-L. Chang and P.A. Thiel, *Phys. Rev. Lett.* **59**, 296 (1987).
- [27] C.R. Brundle, R.J. Behm, and J.A. Barker, *J. Vac. Sci. Technol. A* **2**, 1038 (1984).
- [28] D.-J. Liu and J.W. Evans, *J. Chem. Phys.* **117**, 7319 (2002).
- [29] A.M. Ferrenberg and R.H. Swendsen, *Phys. Rev. Lett.* **61**, 2635 (1988).
- [30] M.N. Barber, in *Phase Transitions and Critical Phenomena*, edited by C. Domb and J.L. Lebowitz (Academic Press, New York, 1983), Vol. 8, pp. 146–268.

- [31] K. Huang, *Statistical Mechanics*, 2nd ed. (Wiley, New York, 1987).
- [32] G. Orkoulas, M.E. Fisher, and A.Z. Panagiotopoulos, *Phys. Rev. E* **63**, 051507 (2001).
- [33] V. Privman and M.E. Fisher, *J. Stat. Phys.* **33**, 385 (1983).
- [34] P. Hanggi, H. Grabert, P. Talkner, and H. Thomas, *Phys. Rev. A* **29**, 371 (1984).
- [35] K.K. Mon and K. Binder, *Phys. Rev. E* **48**, 2498 (1993).
- [36] D.-J. Liu, N. Pavlenko, and J.W. Evans, e-print cond-mat/0304386.
- [37] For the CO oxidation model with $h=2$, one obtains $d_c(L) = 0.0403, 0.0337, 0.0304$, for $L=16, 32, 64$, respectively, consistent with $\nu=1$ (Ising universality), and $d_c(\infty) = 0.0273(2)$.
- [38] N. Pavlenko, J.W. Evans, D.-J. Liu, and R. Imbihl, *Phys. Rev. E* **65**, 016121 (2002).
- [39] J.W. Evans, *J. Chem. Phys.* **97**, 572 (1992).
- [40] J.W. Evans, *J. Chem. Phys.* **98**, 2463 (1993).
- [41] V.P. Zhdanov and B. Kasemo, *Surf. Sci. Rep.* **20**, 111 (1994).